Volume 52 | Number 16 | 25 February 2016 | Pages 3257–3444

ChemComm

Chemical Communications

www.rsc.org/chemcomm

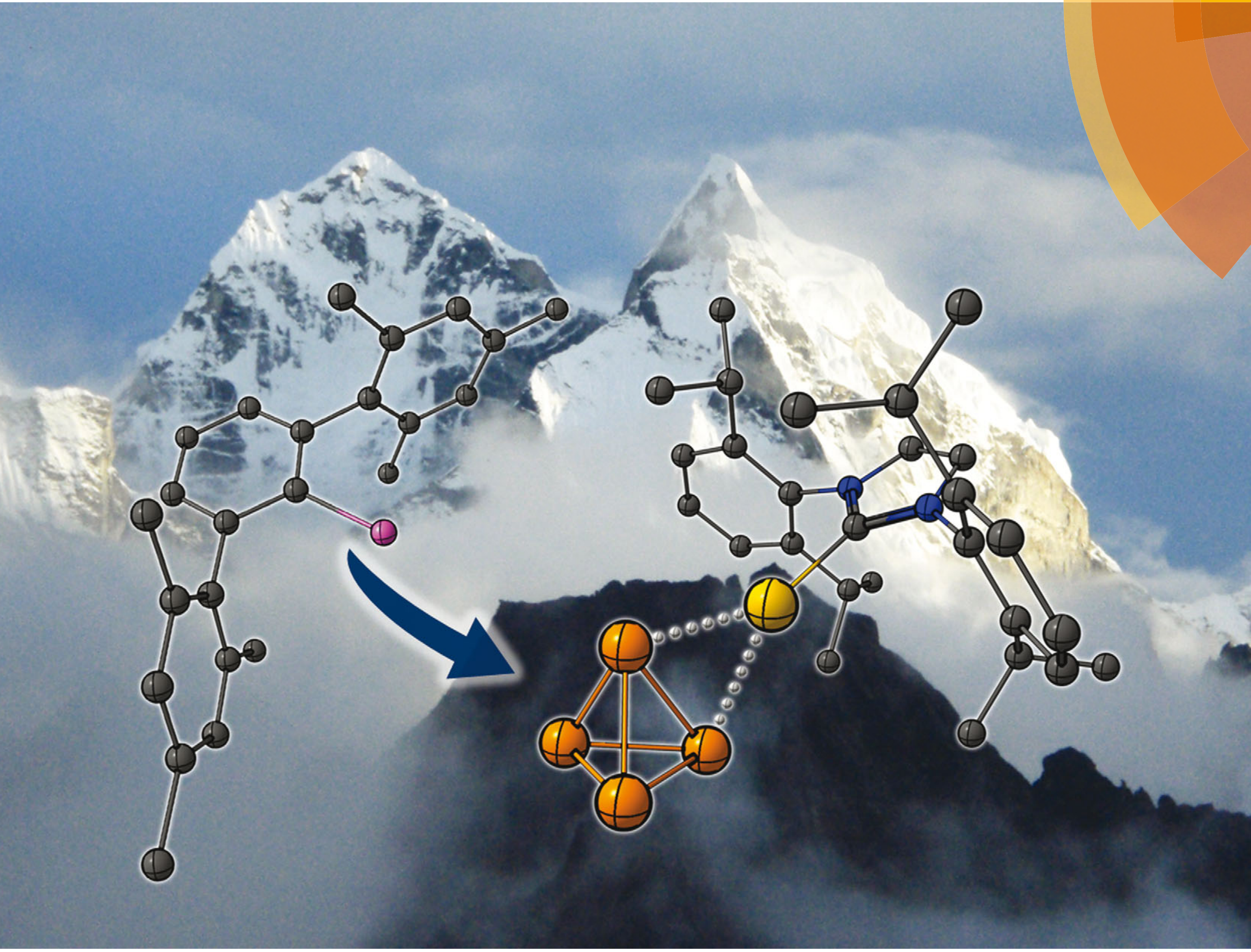

ISSN 1359-7345

ROYAL SOCIETY OF CHEMISTRY

COMMUNICATION

Koop Lammertsma *et al.*

Functionalization of P_4 in the coordination sphere of coinage metal cations

175 YEARS

ChemComm

COMMUNICATION

View Article Online
View Journal | View Issue

Cite this: *Chem. Commun.*, 2016, 52, 3284

Received 6th December 2015,
Accepted 30th December 2015

DOI: 10.1039/c5cc10037b

www.rsc.org/chemcomm

Functionalization of P_4 in the coordination sphere of coinage metal cations†

Jaap E. Borger,[a] Martijn S. Bakker,[a] Andreas W. Ehlers,[a] Martin Lutz,[b] J. Chris Slootweg[a] and Koop Lammertsma*[ac]

Selective functionalization of white phosphorus is achieved by addition of ArLi to unique cationic coinage metal η^2–P_4 complexes. This novel approach allows controlled P–C bond formation using the bulky DmpLi (Dmp = 2,6-$Mes_2C_6H_3$) and the unencumbered MesLi, giving sterically diverse doubly complexed RP_4 butterfly derivatives in a single step.

Controlling direct P–C bond formation using P_4 as starting material is of interest in avoiding chlorinated intermediates, such as PCl_3, for the production of organophosphorus compounds. Yet this task is extremely challenging due to the highly reactive nature of the P_4 tetrahedron.[1] Currently, several selective methods have been developed, like the use of ambiphilic carbenes pioneered by the group of Bertrand,[2] and the metal-mediated radical functionalization of P_4 reported by Scheer *et al.* (**A**; R = Cp^R, Scheme 1)[3] as well as by Cummins and co-workers (R = Dmp),[4] who also demonstrated facile P-functionalization chemistry by embedding photochemically generated P_2 fragments into organic frameworks (**B**).[5] In contrast, conventional methods for the formation of P–C bonds,[6] such as the use of organolithium and Grignard reagents, have been less fruitful due to the low selectivity and complex product distributions associated with their reactions with P_4.[7] An intriguing exception was recently described by Hill, who achieved selective activation of P_4 using a β-diketiminato organomagnesium compound, producing the $[nBu_2P_4]^{2-}$ dianion **C**,[8] which is related to the thallium tetraphosphabutadienediide $[Ar_2P_4]^{2-}$ salt **D** reported by Power *et al.*[9] We showed that the reactivity of bulky ArLi reagents toward P_4 can be controlled in the presence of Lewis acids ($B(C_6F_5)_3$ and BPh_3), giving the LA-stabilized bicyclo[1.1.0]tetraphosphabutanides $[ArP_4{\cdot}LA]^-$ **E** that can subsequently be functionalized selectively generating the neutral disubstituted bicyclic phosphanes ArP_4R (type **A**) and the doubly coordinated tetraphosphides $[ArP_4{\cdot}(LA)_2]^-$ **F**.[10] Key in this approach is the irreversible formation of the transient phosphide $[RP_4]^-$ that is directly trapped by the Lewis acid. Note that P_4 does not form an adduct with BPh_3 or even $B(C_6F_5)_3$,[10] and therefore requires the use of sterically encumbered FLP-type ArLi/LA combinations to avoid quenching. In this work, we present an alternative strategy by using novel cationic coinage metal based Lewis adducts of P_4 as synthon that now tolerate varied bulk on the ArLi reagents, as demonstrated by the selective addition of Dmp (Dmp = 2,6-dimesitylphenyl) and mesityl lithium, resulting in the formation of unique doubly complexed RP_4 butterfly cations.

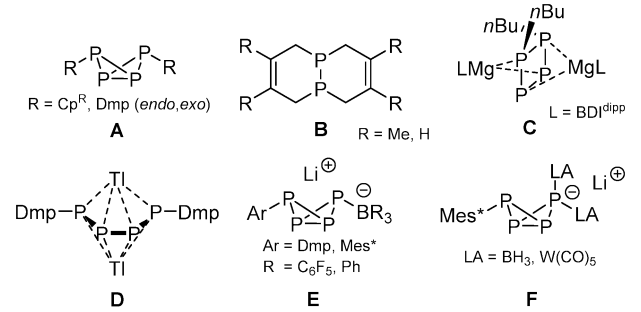

Scheme 1 Methods allowing selective direct P–C bond formation using P_4. Dmp = 2,6-dimesitylphenyl; BDI^{dipp} = $HC\{C(Me)N(2,6\text{-}iPr_2C_6H_3)\}_2$; Mes* = 2,4,6-$tBu_3C_6H_2$; Cp^R = Cp^{BIG}, Cp‴, Cp*, Cp^{4iPr}.

Commercially available IPrMCl (M = Cu, Au; IPr = 1,3-bis(diisopropylphenyl)imidazol-2-ylidene) in combination with Li^+ $[Al(pftb)_4]^-$ (pftb = perfluoro-*tert*-butoxy)[11,12] as chloride scavenger were found to be suitable starting materials allowing the isolation of readily available LA–P_4 adducts. The complexation of P_4 was achieved by dropwise addition of a solution of IPrMCl (1 equiv.; M = Cu, Au) in DCM to a suspension of white phosphorus (1.1 equiv.) and $Li[Al(pftb)_4]$ (1 equiv.) in DCM at 0 °C (Scheme 2), which

---

[a] *Department of Chemistry and Pharmaceutical Sciences Vrije Universiteit Amsterdam, De Boelelaan 1083, 1081 HV Amsterdam, The Netherlands. E-mail: K.Lammertsma@vu.nl*

[b] *Crystal and Structural Chemistry, Bijvoet Center for Biomolecular Research, Utrecht University, Padualaan 8, 3584 CH Utrecht, The Netherlands*

[c] *Department of Chemistry, University of Johannesburg, Auckland Park, Johannesburg, 2006 South Africa*

† Electronic supplementary information (ESI) available. CCDC 1440355 and 1440356. For ESI and crystallographic data in CIF or other electronic format see DOI: 10.1039/c5cc10037b

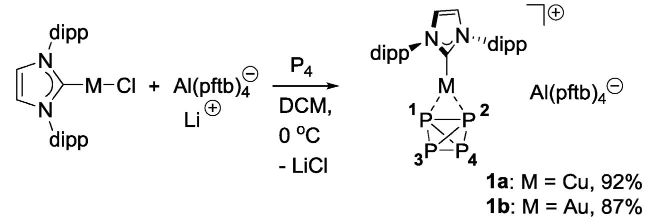

Scheme 2 Synthesis of cationic η^2–P_4 complexes of copper and gold (pftb = $OC(CF_3)_3$; dipp = 2,6-diisopropylphenyl).

resulted in a sharp downfield shifted singlet in the $^{31}P\{^1H\}$ NMR spectrum in the case of Cu(I) (−483.1 ppm), and a lower field and broadened singlet for Au(I) (−464.4 ppm), indicating both P_4 tetrahedra to be coordinated dynamically to the cationic metal centers (free P_4 in CD_2Cl_2: −522.0 ppm). The dynamics were confirmed by VT NMR spectroscopy at −90 °C,[13] revealing broadening of the ^{31}P signal for Cu–P_4 complex **1a**, and two broad triplets for Au–P_4 analogue **1b** (δ ^{31}P: −453.3 and −462.1 ppm, 2 : 2 ratio; $^1J_{P,P}$ = −209.8 Hz). Both novel complexes were isolated as white powders in 92% (**1a**) and 87% (**1b**) yield, respectively, and are unique examples of heteroleptic cationic P_4 coinage metal complexes, complementing the homoleptic series $[M(\eta^2\text{–}P_4)_2]^+$ reported by Krossing[14a–d] (M = Ag, Cu) and Slattery *et al.*[14e] (M = Au), and the neutral copper complex [NacnacCu(η^2–P_4)] isolated by Scheer and coworkers.[14f]

The A_2B_2 spin-system of gold(I) complex **1b** observed at low temperature by ^{31}P NMR spectroscopy is indicative of η^2–P_4 coordination, which was confirmed by a single-crystal X-ray analysis (Fig. 1)[15] that showed nearly equal Au1–P1 (2.4043(17) Å) and Au1–P2 distances (2.4286(19) Å), a distorted trigonal planar Au center with a short Au1–C1 bond (2.037(5) Å), and an acute P1–Au1–P2 angle (57.79(7)°). A comparison of the P–P bonds in "free" P_4 (2.1994(3) Å, determined by gas-phase electron diffraction[16]) with those in **1b**$^+$ shows a contraction of the P3–P4 bond (2.148(3) Å), as well as shortened P1/P2–P3/P4 bonds (2.155(3)–2.167(4) Å), but an elongated P1–P2 bond (2.335(3) Å) due to coordination to gold, albeit less pronounced than the one found in $[Au(\eta^2\text{–}P_4)_2][GaCl_4]$ (*i.e.* 2.410(1) Å[14e]).

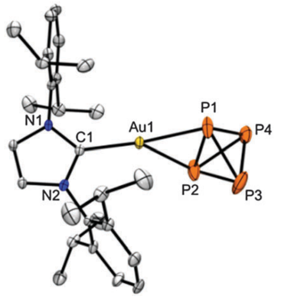

Fig. 1 Molecular structure of **1b**$^+$ in the crystal[15] (ellipsoids are set at 50% probability; $[Al(OC(CF_3)_3)_4]^-$ counter-ion and CH_2Cl_2 solvent molecule omitted). Selected bond lengths [Å] and angles [°]: P1–P2 (2.335(3)), P3–P4 (2.148(3)), P1–P3/P4 (2.167(4)/2.164(3)), P2–P3/P4 (2.156(4)/2.155(3)), Au1–P1/P2 (2.4043(17)/2.4286(19)), C1–Au1 (2.037(5)); C1–Au1–P1 (156.75(14)), C1–Au1–P2 (141.92(14)), P1–Au1–P2 (57.79(7)).

To analyze the bonding situation of **1** in more detail, we resorted to AIM analyses[17,18] on the gas-phase optimized structures of **1a**$^+$ and **1b**$^+$,[19] which revealed bond critical points (BCP) between P1 and P2 (ρ = 0.079 a.u. (ε = 1.10) in **1a**$^+$ and 0.074 a.u. (ε = 0.93) in **1b**$^+$) with only a slightly lower electron density compared to that computed for the naked P_4 (ρ = 0.105 a.u.; ε = 0.10),[13] confirming the coordinating P_4 fragments to remain intact, disfavoring oxidative addition by P–P bond cleavage. Interestingly, examination of the Laplacian of the electron densities ($\nabla^2\rho$) in the P1–P2 BCPs indicated a stronger P_4–M^+ interaction in gold complex **1b**$^+$ (0.056 a.u.) than in Cu derivative **1a**$^+$ (0.033 a.u.), which is in agreement with the observed $^{31}P\{^1H\}$ NMR shifts (−483.1 *vs.* −464.4 ppm for **1a** and **1b**, respectively). ETS-NOCV[20] analyses of the M^+–P_4 bonds concur with these observations,[18] revealing indeed a higher bonding energy for the Au complex ($\Delta\Delta E$ = 1.2 kcal mol^{-1}), with the most prominent difference found for the orbital interactions, showing larger contributions for σ donation (**1b**$^+$ −36.7; **1a**$^+$ −25.9 kcal mol^{-1}) and concurrent π back-donation (**1b**$^+$ −21.4; **1a**$^+$ −20.7 kcal mol^{-1}), attributable to the influence of relativistic effects on the valence shell of Au(I).[21,22]

This difference in bonding energy is also reflected in the stability of **1a** *vs.* **1b**. Namely, dissolving **1a** in toluene directly led to complete displacement of P_4 at room temperature, whereas **1b** is indefinitely stable under those conditions,[23] rendering Au complex **1b** a suitable building block for the functionalization of P_4. As proof of concept, we first selected the bulky DmpLi to react with **1b**, which proved successful in the synthesis of the LA-stabilized Li^+ $[DmpP_4{\cdot}B(C_6F_5)_3]^-$.[10a] Hence, a solution of DmpLi (1 equiv.) in toluene was slowly added to a solution of **1b** (1 equiv.) in toluene at −78 °C, revealing an AMX_2 spin system in the $^{31}P\{^1H\}$ NMR spectrum (−105.5 (P1), −118.7 (P4) and −327.9 (P2, P3) ppm in a 1 : 1 : 2 ratio, respectively), indicative for a non-symmetrically substituted P_4 butterfly.[10,25] Interestingly, ^1H NMR analysis revealed the presence of two NHC moieties instead of only one needed for the anticipated neutral $DmpP_4AuIPr$ **2** (Scheme 3), which suggests the formation of a doubly coordinated RP_4 complex.

Indeed, X-ray crystal structure determination of colorless crystals obtained by layering a DCM solution with *n*-pentane, displayed the non-symmetrical $[DmpP_4{\cdot}(AuIPr)_2][Al(pftb)_4]$ **3** (Fig. 2) featuring a unique bimetallic gold fragment, with similar P4–Au1/Au2 distances (2.2924(7)/2.2860(7) Å) and a Au1–P4–Au2 angle of 128.02(3)°, which is larger than found in the triaurated cation $[RP(AuPPh_3)_3]^+$ (av. 106°),[24] likely due to the steric repulsion between the large NHC ligands. The P4–P2/P3 bonds (2.1919(10)/2.2077(10) Å) are slightly contracted compared to the P1–P2/P3 bonds (2.2140(10)/2.2240(11) Å), and are similar in length to the bridgehead P2–P3 bond (2.1992(11) Å). These structural parameters are akin to those reported for the cationic $[Mes^*{}_2P_4Cl]^+$ of Schulz *et al.*[25a] as well as to those of the bis-LA complexed anions $[Mes^*P_4{\cdot}(LA)_2]^-$ (LA = BH_3, $W(CO)_5$) reported by us.[10b] Intriguingly, the bicyclic P_4 entity in **3**$^+$ is sterically highly shielded, as illustrated by a space-filling model (Fig. 2, right), reminiscent of the incorporation of white phosphorus in the self-assembled $[Fe_4L_6]^{8+}$ container reported by Nitschke and co-workers.[26]

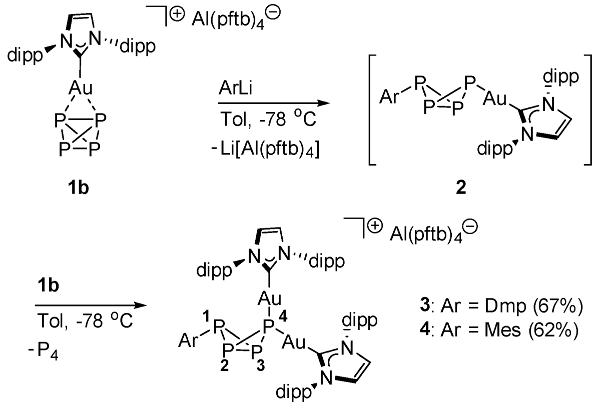

Scheme 3 Functionalization of P_4 by reaction of ArLi with **1b**, with the proposed intermediate **2** in brackets (pftb = $OC(CF_3)_3$; dipp = 2,6-diisopropylphenyl).

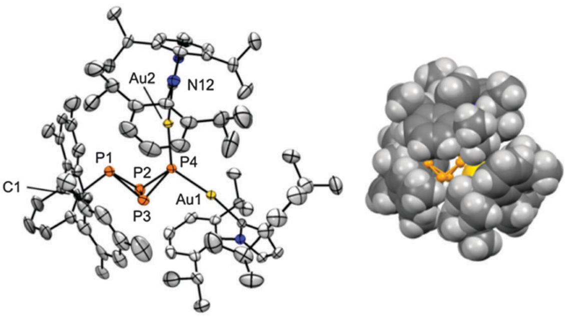

Fig. 2 Left: Molecular structure of $\mathbf{3}^+$ in the crystal[15] (ellipsoids are set at 50% probability; $[Al(OC(CF_3)_3)_4]^-$ counter-ion and disordered solvent molecules omitted). Selected bond lengths [Å], angles and torsion angle [°]: P1–P2/P3 (2.2140(10)/2.2240(11)), P4–P2/P3 (2.1919(10)/2.2077(10)), P2–P3 (2.1992(11)), Au1–P4 (2.2924(7)), Au2–P4 (2.2860(7)), C13–P1 (1.865(3)); Au1–P4–Au2 (128.02(3)); P1–P2–P3–P4 (100.98(4)). Right: Space-filling model of $\mathbf{3}^+$.

The formation of **3** could be optimized by using two equivalents of **1b**, which allowed its isolation in 67% yield. Bis-gold complex **3** is likely formed *via* neutral *exo*,*exo*-ArP_4AuIPr **2** (Scheme 3) that displaces a P_4 molecule from a second equivalent of gold complex **1b**, which was computed to be energetically favorable by -43.1 kcal mol^{-1},[27] and acts as a monodentate ligand (*via* P4) for $[IPrAu]^+$, displaying reactivity analogous to the recent coordination of bicyclic $Mes^*{}_2P_4$ to $GaCl_3$[25b] shown by Schulz *et al.*, and of $[\{Cp'''Fe(CO)_2\}_2(\mu,\eta^{1:1}\text{-}P_4)]$ toward $[Cu(MeCN)]^+$ presented by the group of Scheer.[28]

Next, we assessed the reactivity of **1b** toward the less encumbered nucleophile MesLi,[29] which was not feasible in our original approach (**E**, Scheme 1)[10] as combining MesLi with P_4 in the presence of BPh_3 exclusively produces Li^+ $[MesBPh_3]^-$.[13] Gratifyingly, formation of the bicyclic tetraphosphane $[MesP_4{\cdot}(AuIPr)_2][Al(pftb)_4]$ (**4**) proceeded readily upon mixing MesLi and **1b** (2 equiv.) in toluene at -78 °C, showing a distinct set of three $^{31}P\{^1H\}$ resonances at -110.6 (P1), -119.9 (P4) and -314.5 (P2, P3) ppm (1 : 1 : 2 ratio), and an additional signal for free P_4. The product could be isolated in 62% yield, and was confirmed to contain only one mesityl unit by mass spectrometry (ESI) and ^1H NMR spectroscopy, and two flanking IPrAu moieties.[13] In contrast to related $Aryl_2P_4$ species, which feature either bulky 2,4,6-$t\mathrm{Bu}_3C_6H_3$ (Mes*)[7c,10,25a,b] or terphenyl[4,9,10a] groups, **4** is the first example of a mesityl-substituted P_4 butterfly, which illustrates the merit of this novel P_4-functionalization strategy in controlling direct P–C bond formation using organolithium reagents.

In summary, addition of Dmp or mesityl lithium to the coinage metal based P_4–LA adduct **1b** gives the unique bimetallic ArP_4-butterfly cations **3** and **4**. This novel approach allows for varied bulk on the organosubstituents in a single controlled step, showing facile functionalization of P_4. Currently, we are defining the scope of this new methodology and are exploring the application of **1** in new P_4 transformations.

Notes and references

1 For reviews, see: (*a*) N. A. Giffin and J. D. Masuda, *Coord. Chem. Rev.*, 2011, **255**, 1342; (*b*) B. M. Cossairt, N. A. Piro and C. C. Cummins, *Chem. Rev.*, 2010, **110**, 4164; (*c*) M. Caporali, L. Gonsalvi, A. Rossin and M. Peruzzini, *Chem. Rev.*, 2010, **110**, 4178; (*d*) M. Scheer, G. Balázs and A. Seitz, *Chem. Rev.*, 2010, **110**, 4236; (*e*) M. Peruzzini, L. Gonsalvi and A. Romerosa, *Chem. Soc. Rev.*, 2005, **34**, 1038.
2 (*a*) J. D. Masuda, W. W. Schoeller, B. Donnadieu and G. Bertrand, *Angew. Chem., Int. Ed.*, 2007, **46**, 7052; (*b*) O. Back, G. Kuchenbeiser, B. Donnadieu and G. Bertrand, *Angew. Chem., Int. Ed.*, 2009, **48**, 5530; (*c*) C. D. Martin, C. M. Weinstein, C. E. Moore, A. L. Rheingold and G. Bertrand, *Chem. Commun.*, 2013, **49**, 4486; (*d*) C. L. Dorsey, B. M. Squires and T. W. Hudnall, *Angew. Chem., Int. Ed.*, 2013, **52**, 4462.
3 S. Heinl, S. Reisinger, C. Schwarzmaier, M. Bodensteiner and M. Scheer, *Angew. Chem., Int. Ed.*, 2014, **53**, 7639.
4 B. M. Cossairt and C. C. Cummins, *New J. Chem.*, 2010, **34**, 1533.
5 D. Tofan and C. C. Cummins, *Angew. Chem., Int. Ed.*, 2010, **49**, 7516.
6 D. E. C. Corbridge, *Phosphorus*, Elsevier, Amsterdam, 2000.
7 (*a*) M. M. Rauhut and A. M. Semsel, *J. Org. Chem.*, 1963, **28**, 471; (*b*) M. M. Rauhut and A. M. Semsel, *J. Org. Chem.*, 1963, **28**, 473; (*c*) R. Riedel, H.-D. Hausen and E. Fluck, *Angew. Chem., Int. Ed.*, 1985, **24**, 1056.
8 M. Arrowsmith, M. S. Hill, A. L. Johnson, G. Kociok-Köhn and M. F. Mahon, *Angew. Chem., Int. Ed.*, 2015, **54**, 7882.
9 A. R. Fox, R. J. Wright, E. Rivard and P. P. Power, *Angew. Chem., Int. Ed.*, 2005, **117**, 7907.
10 (*a*) J. E. Borger, A. W. Ehlers, M. Lutz, J. C. Slootweg and K. Lammertsma, *Angew. Chem., Int. Ed.*, 2014, **53**, 12836; (*b*) J. E. Borger, A. W. Ehlers, M. Lutz, J. C. Slootweg and K. Lammertsma, *Angew. Chem., Int. Ed.*, 2016, **55**, 613.
11 I. Krossing, *Chem. – Eur. J.*, 2001, **7**, 490.
12 I. Krossing and I. Raabe, *Angew. Chem., Int. Ed.*, 2004, **43**, 2066.
13 See the ESI,† for further details.
14 (*a*) I. Krossing, *J. Am. Chem. Soc.*, 2001, **123**, 4603; (*b*) I. Krossing and L. van Wüllen, *Chem. – Eur. J.*, 2002, **8**, 700; (*c*) A. Bihlmeier. M. Gonsior, I. Raabe, N. Trapp and I. Krossing, *Chem. – Eur. J.*, 2004, **10**, 5041; (*d*) G. Santiso-Quiñones, A. Reisinger, J. Slattery and I. Krossing, *Chem. Commun.*, 2007, 5046; (*e*) L. C. Forfar, T. J. Clark, M. Green, S. M. Mansell, C. A. Russell, R. A. Sanguramath and J. M. Slattery, *Chem. Commun.*, 2012, **48**, 1970; (*f*) F. Spitzer, M. Sierka, M. Latronico, P. Mastrorilli, A. V. Virovets and M. Scheer, *Angew. Chem., Int. Ed.*, 2015, **54**, 4392.
15 CCDC 1440355 (compound **1b**) and 1440356 (compound **3**) contain the supplementary crystallographic data for this paper.
16 B. M. Cossairt, C. C. Cummins, A. R. Head, D. L. Lichtenberger, R. J. F. Berger, S. A. Hayes, N. M. Mitzel and G. Wu, *J. Am. Chem. Soc.*, 2010, **132**, 8459.
17 R. F. W. Bader, *Atoms in Molecules*, Claredon Press, Oxford, 1994.
18 The AIM and ETS-NOCV analysis was performed at ZORA-BP86-D3/TZ2P using ADF2013.01; see the ESI,† for details.
19 Geometry optimizations were performed at ωB97X-D/6-31+G(2d,p) (LanL2DZ for Cu and Au); J.-D. Chai and M. Head-Gordon, *Phys. Chem. Chem. Phys.*, 2008, **10**, 6615; see the ESI,† for details.

20 M. P. Mitoraj, A. Michalak and T. Ziegler, *J. Chem. Theory Comput.*, 2009, **5**, 962.

21 This trend was also found in a computational study on homoleptic P_4 complexes of group 11 cations: H.-C. Tai, I. Krossing, M. Seth and D. V. Deubel, *Organometallics*, 2004, **23**, 2343.

22 (*a*) P. Pyykkö, *Chem. Rev.*, 1988, **88**, 563; (*b*) P. Pyykkö, *Angew. Chem., Int. Ed.*, 2004, **43**, 4412.

23 Direct dissociation was observed for both complexes in Et_2O, THF and MTBE.

24 H. Schmidbaur, G. Weidenhiller and O. Steigelmann, *Angew. Chem., Int. Ed.*, 1991, **30**, 433.

25 Selected examples: (*a*) J. Bresien, K. Faust, A. Schulz and A. Villinger, *Angew. Chem., Int. Ed.*, 2015, **54**, 6926; (*b*) J. Bresien, K. Faust, C. Hering-Junghans, J. Rothe, A. Schulz and A. Villinger, *Dalton Trans.*, 2016, DOI: 10.1039/C5DT02757H; (*c*) D. Holschumacher, T. Bannenberg, K. Ibrom, C. G. Daniliuc, P. G. Jones and M. Tamm, *Dalton Trans.*, 2010, **39**, 10590; (*d*) M. B. Power and A. R. Barron, *Angew. Chem., Int. Ed.*, 1991, **30**, 1353.

26 P. Mal, B. Breiner, K. Rissanen and J. R. Nitschke, *Science*, 2009, **324**, 1697.

27 To reduce the computation time, all aryl substituents were replaced by phenyl groups. DFT calculations were performed at ωB97X-D/6-311+G(2d,p)//6-31G(d)(LanL2DZ for Au) using Gaussian09 (Revision D.01); see the ESI,† for details.

28 C. Schwarzmaier, S. Heinl, G. Balázs and M. Scheer, *Angew. Chem., Int. Ed.*, 2015, **54**, 13116.

29 Lerner *et al.* isolated $[Li_3][Mes_3P_4]$ by reaction of P_4 with 3 equiv. of MesLi: A. Hübner, T. Bernert, I. Sänger, E. Alig, M. Bolte, L. Fink, M. Wagner and H.-W. Lerner, *Dalton Trans.*, 2010, **39**, 7528.